

# SYSTEMATIC STUDIES OF FISSION FRAGMENT DE-EXCITATION BY PROMPT $\gamma$ -RAY EMISSION\*

ANDREAS OBERSTEDT

Extreme Light Infrastructure–Nuclear Physics (ELI–NP)  
Horia Hulubei National Institute for Physics and Nuclear Engineering (IFIN–HH)  
077125 Bucharest–Măgurele, Romania

ANGÉLIQUE GATERA, ALF GÖÖK, STEPHAN OBERSTEDT

European Commission, DG Joint Research Centre  
Directorate G — Nuclear Safety and Security  
Unit G.2 — Standards for Nuclear Safety, Security and Safeguards  
2440 Geel, Belgium

*(Received February 14, 2019)*

In recent measurements of prompt  $\gamma$  rays from the spontaneous fission of  $^{252}\text{Cf}$ , the focus was put on the study of angular correlations between  $\gamma$  rays and the nuclei from which they were emitted, and the dependence between prompt fission  $\gamma$ -ray characteristics and fission fragment mass, respectively. First preliminary results are presented and compared to results from other experiments as well as from model calculations.

DOI:10.5506/APhysPolB.50.275

## 1. Introduction

The energy release in nuclear fission is distributed in kinetic and excitation energy of the two fragments. The latter manifests itself in fragment deformation and intrinsic excitation energy. In an early and quite simplified picture, it was assumed that the fragments are first de-excited by the emission of neutrons until the fragments' remaining excitation energy is lower than the neutron binding energy, *i.e.* on average at about half of it. Only then de-excitation would continue by the emission of  $\gamma$  rays, eventually reaching the ground state [1]. These  $\gamma$  rays may be divided into two categories, commonly called statistical and discrete  $\gamma$  rays, respectively. The

---

\* Presented at the Zakopane Conference on Nuclear Physics “Extremes of the Nuclear Landscape”, Zakopane, Poland, August 26–September 2, 2018.

first ones originate mainly from electric dipole transitions and carry away most of the remaining excitation energy of the fragments, while the latter stem mainly from electric quadrupole transitions along the yrast line and carry away most of the angular momentum of the fragments [2]. This so-called prompt  $\gamma$ -ray emission is a fast process, which basically takes place within the first few nanoseconds after scission [3] and is followed by  $\beta$  decay(s), and thereafter by delayed emission of neutrons and  $\gamma$  rays towards the valley of  $\beta$  stability. The average prompt fission  $\gamma$ -ray multiplicity, *i.e.* the average number of photons per fission, amounts typically to eight [4], as corroborated by our previous measurements [5–10]. Figure 1 shows the part of the Nuclear Chart that contains the compound systems investigated so far as well as upcoming projects, together with the cause of fission, *i.e.* spontaneous or induced.

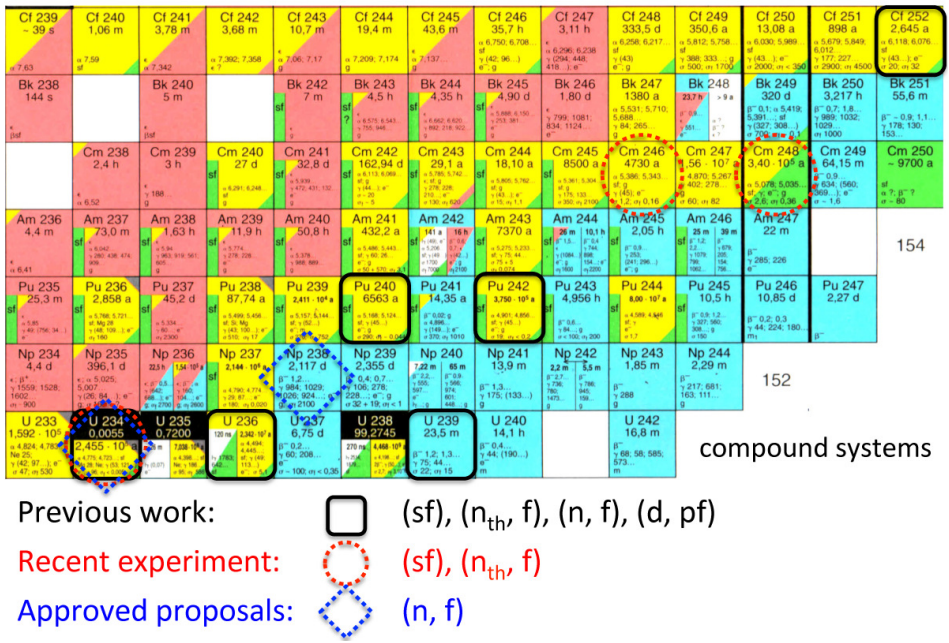


Fig. 1. Overview of compound systems, whose fission process was investigated by us during the past years as well as ongoing and planned work. Here, it is also indicated, whether it was spontaneous or induced fission, and in the case of the latter which reaction was employed.

The comparison of prompt fission  $\gamma$ -ray spectrum (PFGS) characteristics from different fissioning systems makes it possible to establish and/or to refine systematics, which allows estimating prompt fission  $\gamma$ -ray characteristics for systems that are difficult or even impossible to study experimen-

tally. Based on this systematics, a quite simple model allows to predict these characteristics for different excitation energies, as recently demonstrated for  $^{238}\text{U} + n$  [11]. Results from experiments with different probes and/or at different incident energies [12–14] are in rather good agreement with our calculated values. An overview on our past and future activities within this field of research is also given in Ref. [15].

In this paper, we report on the first preliminary results from recent measurements of prompt  $\gamma$ -ray spectra from  $^{252}\text{Cf}(\text{sf})$ , in which the focus is put on the measurement of angular correlations between fission fragments and prompt  $\gamma$  rays, and the dependence of prompt fission  $\gamma$ -ray characteristics from the mass (or rather mass bin) of the fission fragments, respectively.

## 2. Angular correlation measurement

This measurement was performed with a 76.2 mm  $\times$  76.2 mm (diameter  $\times$  length) LaBr<sub>3</sub>:Ce scintillation detector that was placed perpendicular to the plane of the  $^{252}\text{Cf}$  sample along its symmetry axis. This experimental setup allowed measuring the angular distribution of prompt  $\gamma$  rays, in order to study the de-excitation of fission fragments by prompt  $\gamma$ -ray emission and to deduce information about the relative contributions from radiation of different multipolarity. The sample was mounted inside a cylindrical twin Frisch-grid ionization chamber (FGIC) [17] in the center of a common cathode. Fission fragments from a thin  $^{252}\text{Cf}$  sample are emitted to both sides of the cathode, ionizing the P-10 counting gas, and being detected by means of the electrons moving towards the respective anodes. A Frisch grid is placed in front of each anode in order to shield the latter from the influence of the ions, but it also allows determining the (polar) emission angle of the fragments. The FGIC provides the fission trigger for the coincident measurement of  $\gamma$  rays, for which energy and time-of-flight (TOF) between sample and detector are recorded. The latter information is used to distinguish prompt  $\gamma$  rays from other photons, emitted *e.g.* in prompt fission neutron induced reactions, *i.e.* mainly inelastic neutron scattering. The experimental techniques applied here are, in principle, the same as described in Refs. [5–10], where more details may be found.

The collected prompt fission  $\gamma$  rays were sorted into energy spectra for  $\cos\theta$  bins between 0 and 1 in steps of 0.05. In order to obtain emission spectra, the response function of the detector has to be determined, which is usually done by means of Monte Carlo simulations of the actual setup with computer codes like *e.g.* Penelope [18] or Geant4 [19]. Thereafter the response function must be unfolded from the raw spectra. However, as a first step, we have chosen here a different, less time-consuming approach. Adding up all spectra gives an angular integrated raw spectrum that may

be compared with others, obtained previously for the same fissioning system. Since they all turned out to exhibit a very similar appearance, we may benefit from the fact that similar raw spectra lead to similar emission spectra, provided that detector and setup are comparable [7]. This is the case here. From a previous measurement [5], for which the proper unfolding was carried out, both measured and emission spectra are known, whose ratio gives a transformation function (see Ref. [7] for details). Multiplying this function with the recently measured PFGS gives then the emission spectrum. In the same way, angular-dependent emission spectra were created for each bin, from which PFGS characteristics were determined. A detailed inspection of the obtained angular distribution is performed below.

As described above, emission spectra of prompt fission  $\gamma$  rays were created for  $\cos\theta$  bins, covering the polar angle range of  $0^\circ < \theta < 90^\circ$ . The integrated total multiplicity, *i.e.* the average number of emitted photons per fission, was determined to  $\overline{M}_\gamma = 8.28 \pm 0.51$ , where the statistical uncertainty is 0.07 and the systematic one, mainly due to the transformation function, amounts to 0.44. This result is in good agreement with our last published value  $\overline{M}_\gamma = 8.29 \pm 0.13$  [6]. The angular distribution of radiation may be expressed according to

$$W(\theta) = A_0[1 + \{A_2/A_0\}P_2(\cos\theta) + \{A_4/A_0\}P_4(\cos\theta)], \quad (1)$$

where  $P_k(\cos\theta)$  denote Legendre polynomials for  $k = 2, 4$  and  $\theta$  is the emission angle of the fission fragment relative to the  $\gamma$ -ray direction, *i.e.* perpendicular to the cathode plane of the FGIC. Any possible attenuation coefficients are assumed to be 1. The coefficients  $\{A_k/A_0\}$  are determined experimentally and may be compared to theory for different types of radiation. For instance,  $\{A_2/A_0\} \approx -0.3$  for pure dipole radiation and  $\{A_2/A_0\} \approx +0.3$  for pure quadrupole radiation, while  $\{A_4/A_0\}$  is close to zero [20]. The obtained coefficient is  $\{A_2/A_0\} = 0.13 \pm 0.03$ , which may be considered as the result of a superposition of dipole and quadrupole photons (higher multiplicities are less probable and neglected here). Accordingly, it follows that  $(+0.3) \times p + (-0.3) \times (1 - p) = 0.13$ , with  $p$  denoting the probability for quadrupole radiation. This leads to  $p = 0.72$ , corresponding to 72% quadrupole ( $L = 2$ ) and 28% dipole ( $L = 1$ ) radiation.

In the next step, we tried to assess how the ratio between quadrupole and dipole radiation depends on the energy of the prompt fission  $\gamma$  rays. For that reason, the PFGS was rebinned into 500 keV intervals, for which the corresponding angular distributions were fitted according to Eq. (1) as described above for the entire spectrum. As a consequence, the coefficient  $\{A_2/A_0\}$  was determined for each energy bin and the contributions for  $L = 1$  and  $L = 2$  deduced. More detailed information may be found in Ref. [21].

The obtained fitted angular distributions for both the entire energy spectrum and the individual energy bins are shown in Fig. 2. Although it needs to be stated that statistics deteriorates with increasing  $\gamma$ -ray energy due to the exponentially decreasing slope of the spectra, the differences in the angular distributions indicate clearly that dipole and quadrupole radiation exhibit different energy spectra, which should be reflected in their respective characteristics. The corresponding results are shown in Table I, which apart from our — preliminary — experimental values contains even results from calculations with the Monte Carlo Hauser–Feshbach code FIFRELIN [16]. Being rather successful in reproducing experimental results for PFGS characteristics as well as the distinct peak structure of the low-energy part of the energy spectra for  $^{235}\text{U}(n_{\text{th}}, f)$  [8] and  $^{252}\text{Cf}(sf)$  [6], also multipolarity-dependent spectra were generated [22]. However, here it must be noted that, apart from  $\gamma$  rays of known multipolarity 1 and 2, there is a considerable amount of photons, whose multipolarity is not assigned (denoted with “experimental” in Table I), since they correspond to transitions between levels taken from the RIPL-3 database [23]. In fact, they constitute about 44% of the calculated total average PFGS multiplicity. Since a dominating contribution of quadrupole radiation has been observed even in other PFGS

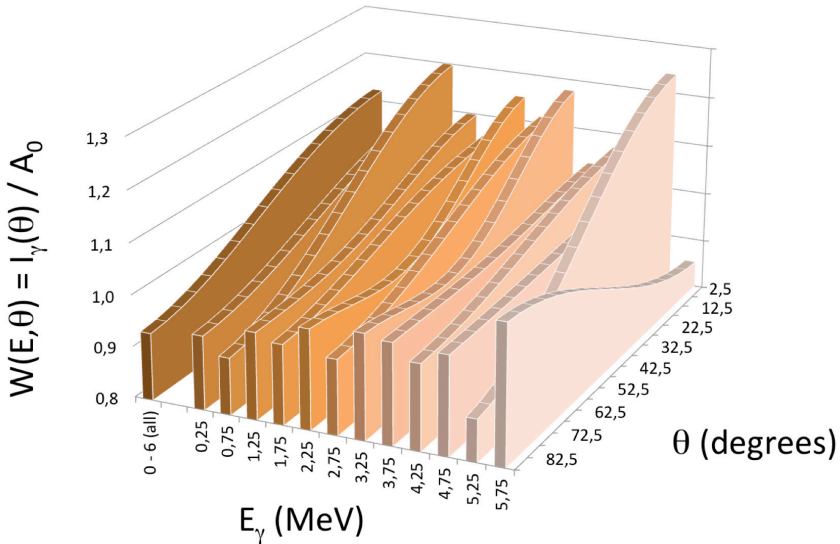


Fig. 2. Pseudo-3D plot of the fit results to the measured angular distributions of prompt  $\gamma$  rays from  $^{252}\text{Cf}(sf)$  according to Eq. (1). Shown is the angular distribution obtained for the entire energy spectrum to the left together with those for the individual energy bins. Please, observe that for the latter, the axis description gives the center of each bin.

measurements (see *e.g.* Refs. [24, 25]), we tend to conclude that most of these transitions of unknown multipolarity should lead to quadrupole radiation. Therefore, the sum of these “experimental” transitions and the calculated ones with  $L = 2$  should be compared to the experimentally obtained contribution for  $L = 2$ . With this condition comparison of the values given Table I shows indeed rather good agreement.

TABLE I

Prompt  $\gamma$ -ray characteristics for the spontaneous fission of  $^{252}\text{Cf}$ . Experimental results from this work for the average  $\gamma$ -ray multiplicity  $\overline{M}_\gamma$ , the average energy per photon  $\epsilon_\gamma$ , and the total energy  $E_{\gamma,\text{tot}}$  released in fission, are given for the integral spectrum as well as for the multipolarity-dependent spectra and compared to corresponding values recently calculated with FIFRELIN [22] (see the text for details). Relative multiplicities are also given, under the assumption that higher multiplicities may be neglected.

Multipolarity $L$		Experiment (this work)	Calculations (FIFRELIN)
$\overline{M}_\gamma$	all	$8.28 \pm 0.51$	8.28 (adjusted)
$\overline{M}_\gamma$	1	2.31	3.20 (39%)
$\overline{M}_\gamma$	2	5.97	1.45 (17%)
$\overline{M}_\gamma$	experimental		3.63 (44%)
$\epsilon_\gamma$	all	$0.79 \pm 0.10$ MeV	0.76 MeV
$\epsilon_\gamma$	1	0.86 MeV	0.94 MeV
$\epsilon_\gamma$	2	0.76 MeV	1.03 MeV
$\epsilon_\gamma$	experimental		0.50 MeV
$E_{\gamma,\text{tot}}$	all	$6.51 \pm 0.76$ MeV	6.30 MeV
$E_{\gamma,\text{tot}}$	1	1.99 MeV	3.00 MeV
$E_{\gamma,\text{tot}}$	2	4.52 MeV	1.49 MeV
$E_{\gamma,\text{tot}}$	experimental		1.81 MeV

### 3. Mass-dependent prompt fission $\gamma$ -ray emission

In the second measurement discussed here, PFGS from  $^{252}\text{Cf}$  were measured with two  $\text{LaBr}_3:\text{Ce}$  scintillation detectors of the size of  $50.8 \text{ mm} \times 50.8 \text{ mm}$  (diameter  $\times$  length) which this time were placed in plane with the transparent sample, mounted again on the common cathode inside a double-sided FGIC. The remaining experimental details correspond to those given in Sect. 2. Using the 2E-method, the masses of both fission fragments could be determined, however with a mass resolution not much better than 5 (FWHM). For that reason, but also in order to increase statistics, mass windows were set with bin size  $\Delta A > 1$ , for which PFGS were collected and

their characteristics determined. So far, data from only one of the LaBr<sub>3</sub>:Ce detectors have been analyzed and uncertainties have not been assessed yet. Figure 3 shows first preliminary results for the total  $\gamma$ -ray energy for a pair of fission fragments as a function of the heavy fragments mass. Here, mass bins were chosen with a width of  $\Delta A = 2$  (for both light and heavy fragments), except for most asymmetric fission with  $\Delta A = 14$ . Our work is compared to experimental values from Nifenecker *et al.* [26] and the results from Point-by-Point model calculations [27]. The general agreement between all three sets of data is obviously good, although differences are apparent for symmetric fission; in particular, for Ref. [26],  $E_{\gamma,\text{pair}}$  is much higher in this mass region. The average total  $\gamma$ -ray energy, obtained as the sum of the depicted energies weighted with the fission-fragment mass distribution, is for our results normalized to the previously published value  $E_{\gamma,\text{tot}} = 6.65$  MeV [6], which is in good agreement with 6.68 MeV for the data from Ref. [27]. In contrast, for Ref. [26],  $E_{\gamma,\text{tot}} = 6.83$  MeV is obtained, which may easily be accounted for by the visible enhancement for symmetric fission.

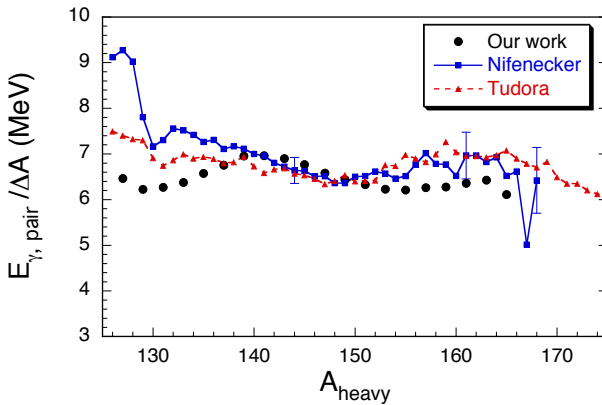


Fig. 3. Total  $\gamma$ -ray energy for a pair of fission fragments as a function of the heavy fragments mass. Our preliminary experimental results, denoted as black dots, were obtained for mass bins  $\Delta A > 1$  due to the limited mass resolution of the FGIC (see the text for details). They are compared to data from Ref. [26] and values calculated with the Point-by-Point model [27], represented by squares and triangles, respectively.

#### 4. Discussion and outlook

In this work, first results have been presented from two PFGS measurements with a <sup>252</sup>Cf source. Although the results must still be considered preliminary, the agreement with other results — experimental and calculated — is good.

As far as the angular distribution of prompt fission  $\gamma$  rays is concerned, this agreement would have been even better, if a probably more realistic assumption for the coefficient for pure dipole radiation,  $\{A_2/A_0\} \approx -0.2$ , had been made, considering the value  $\{A_2/A_0\} = -0.212(26)$  from the example given in Ref. [20]. With this value,  $\overline{M}_{\gamma,L=1} \approx 2.8$  and  $\overline{M}_{\gamma,L=2} \approx 5.5$  would have been obtained, corresponding to relative contributions of 34% and 66%, respectively. This result must be compared with other related information on fission fragments, such as average neutron separation energies and average moments of inertia, in order to verify the deduced energies carried away by dipole and quadrupole photons during the de-excitation process of fission fragments. Concerning the mass dependence of the released  $\gamma$ -ray energy, the full data must still be analyzed; this is in progress. Hence, both activities are to be continued.

One of the authors (A.O.) acknowledges the support from the Extreme Light Infrastructure–Nuclear Physics (ELI–NP) Phase II, a project co-financed by the Romanian Government and the European Union through the European Regional Development Fund — the Competitiveness Operational Programme (1/07.07.2016, COP, ID 1334), with which this work had been finalized.

## REFERENCES

- [1] C. Wagemans (Ed.), *The Nuclear Fission Process*, CRC Press, Boca Raton 1991.
- [2] A. Hotzel *et al.*, *Z. Phys. A* **356**, 299 (1987).
- [3] P. Talou *et al.*, *Phys. Rev. C* **94**, 064613 (2016).
- [4] R. Vandenbosch, J.R. Huizenga, *Nuclear Fission*, Academic Press New York and London 1973.
- [5] R. Billnert, F.-J. Hamsch, A. Oberstedt, S. Oberstedt, *Phys. Rev. C* **87**, 024601 (2013).
- [6] A. Oberstedt, R. Billnert, F.-J. Hamsch, S. Oberstedt, *Phys. Rev. C* **92**, 014618 (2015).
- [7] S. Oberstedt *et al.*, *Phys. Rev. C* **93**, 054603 (2016).
- [8] A. Oberstedt *et al.*, *Phys. Rev. C* **87**, 051602(R) (2013).
- [9] S. Oberstedt *et al.*, *Phys. Rev. C* **90**, 024618 (2014).
- [10] A. Gatera *et al.*, *Phys. Rev. C* **95**, 064609 (2017).
- [11] A. Oberstedt, R. Billnert, S. Oberstedt, *Phys. Rev. C* **96**, 034612 (2017).
- [12] S.J. Rose *et al.*, *Phys. Rev. C* **96**, 014601 (2017).
- [13] L. Qi *et al.*, *Phys. Rev. C* **98**, 014612 (2018).

- [14] J.-M. Laborie *et al.*, *Phys. Rev. C* **98**, 054604 (2018).
- [15] S. Oberstedt *et al.*, *Eur. Phys. J. A* **51**, 178 (2015).
- [16] O. Litaize, O. Serot, *Phys. Rev. C* **82**, 054616 (2010).
- [17] C. Budtz-Jørgensen *et al.*, *Nucl. Instrum. Methods Phys. Res. A* **258**, 209 (1987).
- [18] <http://www.oecd-nea.org/tools/abstract/detail/nea-1525>
- [19] S. Agostinelli and the Geant4 Collaboration, *Nucl. Instrum. Methods Phys. Res. A* **506**, 250 (2003).
- [20] E.S. Paul, UK Nuclear Physics Summer School, Bristol, August 27–September 6, 2013,  
<http://ns.ph.liv.ac.uk/~ajb/summerschool/files/ESP-Lecture4.pdf>
- [21] A. Oberstedt *et al.*, *EPJ Web Conf.* **169**, 00014 (2018).
- [22] A. Chebboubi, private communication, 2017.
- [23] R. Capote *et al.*, *Nucl. Data Sheets* **110**, 3107 (2009).
- [24] M.M. Hoffman, *Phys. Rev.* **133**, B714 (1964).
- [25] Yu.N. Kopach *et al.*, *Phys. Rev. Lett.* **82**, 303 (1999).
- [26] H. Nifenecker *et al.*, *Nucl. Phys. A* **189**, 285 (1972).
- [27] A. Tudora, private communication, 2017.